

## Problems of Secondary Sources for Hybrid Ray Tracing and FEM Simulation

**J. Ziemelis**

*Riga Technical University*

*Azenes iela 12, LV-1048, Riga, Latvia, phone: +371 7089205; fax: +371 7089292; e-mail: ziemelis@rsf.rtu.lv*

### Introduction

The ray tracing is approximate method for simulation the scattering, propagation and penetration of electromagnetic radiation in regions of space large in comparison with radiation wavelength. In many cases it is only one reasonable method for numerical solution of such problems, because known numerical methods as Finite Element Method (FEM) for frequency [1] and time representations (FDTD) [2] are efficient only for regions limited by pair of wavelengths. For simulation the wave propagation in urban and indoor environment the best are hybrid methods with sharing ray tracing method [3]. In spite of combination of different methods the complicated geometry of tasks requires to carry out some simplifications [4]. The specific geometry sometimes allow us to use two - dimensional (2D) simulation [5] instead of three-dimensional (3D) simulation. 2D simulations are often used to compare results given by ray tracing and FE or FDTD methods because for 2D simulation region dimension can be some wavelengths.

Often FE or FDTD methods are applied for calculating the scattered field in small regions (the observation point is located in this region). Still in some cases the scattered field is strong enough for continuation of ray tracing. In these cases the FEM region may be treated as secondary source of radiation. Lately still most hybrids are created on base of FDTD method, but for signals with narrow frequency band FE method has some advantages.

This paper gives a theoretical fundament for creating secondary ray sources of FEM region. For creating ray sources we must determine intensity and orientation of all rays on the boundary of FEM region. To explain the methodology we will use two-dimensional model. This model has following advantages:

- mathematical description and the software is simple;
- comparison of exact and approximate methods is possible;
- drawing of geometry is not complicated.

The 2D simulation can be compared with measurements for cases when electromagnetic field depends only from two co-ordinates or dependence from the third co-ordinate is known. Successfully 2D simulation

can be applied for wave propagation in tunnels or in waveguides.

Because we are interested in field calculation for signals with narrow frequency band the most reasonable method is FEM.

For analysis is selected sinusoidal source with polarisation - TE  $\{H_z, E_x, E_y\}$ .

### Methodology of source creating

Let the FEM region has a shape of cylinder (Fig.1.) with radius  $\rho$ . The scatter is located in this region.

Through region propagate an incident field  $H_z^i$ . The incident field creates the scattered field that outside the FEM region is marked with the Pointing vector. The Pointing vector on the boundary of FEM region determines the intensity and orientation of secondary rays.

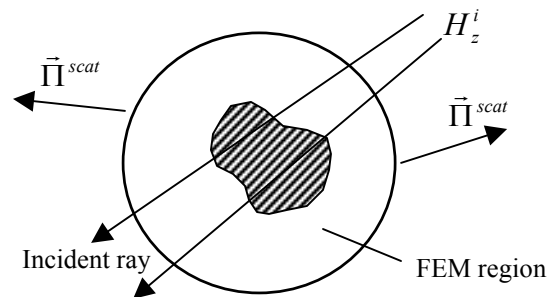


**Fig. 1.** A FEM region with scatter and incident rays

For numerical calculations the FEM region must be covered with mesh. The mesh truncating in this case must be carried out by Boundary Integral (BI) method.

Part of the FEM region is illuminated by incident ray that on Fig.1. is depicted as region between boundary rays. In this region the nonzero incident field will appear in the field equations. For TE wave the vector wave equation (region without current sources) becomes:

$$\nabla_t \times \left[ \frac{1}{\epsilon_r} \nabla_t \times (\vec{e}_z H_z) \right] - \vec{e}_z k_0^2 \cdot \mu_r \cdot H_z = 0, \quad (1)$$

where index  $t$  denotes transversal operator;  $\varepsilon_r$ - relative complex permittivity; for nonmagnetic materials relative permeability can be simplified  $\mu_r = 1$ .

The vector product can be transformed for 2D case to

$$\begin{aligned} \nabla_t \times \left[ \frac{1}{\varepsilon_r} \nabla_t \times (\tilde{\mathbf{e}}_z H_z) \right] &= \nabla_t \times \left[ \frac{1}{\varepsilon_r} (-\tilde{\mathbf{e}}_z \times \nabla_t H_z) \right] = \\ &= -\tilde{\mathbf{e}}_z \nabla_t \cdot \frac{1}{\varepsilon_r} \nabla_t H_z. \end{aligned}$$

This transformation gives for  $H_z$  the scalar equation

$$\nabla_t \cdot \left( \frac{1}{\varepsilon_r} \nabla_t H_z \right) + k_0^2 \cdot H_z = 0.$$

The  $H_z$  field is typically decomposed as a sum from incident and scattered fields:

$$H_z = H_z^i + H_z^{scat}.$$

Now the wave equation for scattered field is

$$\nabla_t \cdot \left( \frac{1}{\varepsilon_r} \nabla_t H_z^{scat} \right) + k_0^2 \cdot H_z^{scat} = f(x, y), \quad (2)$$

where

$$f(x, y) = -\nabla_t \cdot \left( \frac{1}{\varepsilon_r} \nabla_t H_z^i \right) - k_0^2 \cdot H_z^i.$$

The weak form of wave equation for FEM region with square  $\Omega$  and weighting function  $W(x, y)$  is [1]:

$$\begin{aligned} \iint_{\Omega} \left[ -\nabla W(\bar{\mathbf{r}}) \cdot \nabla H_z^{scat}(\bar{\mathbf{r}}) + k_0^2 \cdot \varepsilon_r \cdot W(\bar{\mathbf{r}}) \cdot H_z^{scat}(\bar{\mathbf{r}}) \right] \cdot ds + \\ + \int_C W(\bar{\mathbf{r}}) \cdot [\bar{\mathbf{n}} \cdot \nabla H_z^{scat}(\bar{\mathbf{r}})] \cdot dl = \iint_{\Omega} W(\bar{\mathbf{r}}) \cdot f(\bar{\mathbf{r}}) \cdot ds \end{aligned}$$

For numerical calculations all FEM region is covered with mesh from  $N_e$  triangular elements. Every local triangle has unique element identification and three local nodes, which are at the same time global nodes (Fig.2). Numeration of local nodes is always counter-clockwise.

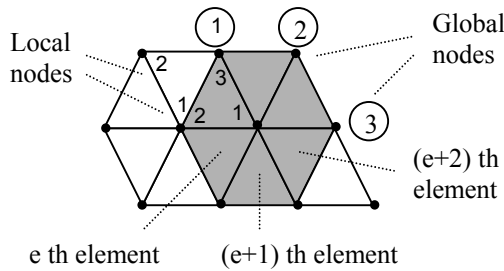


**Fig. 2.** Triangular node based mesh elements, local and global nodes

The scattered field may be represented

$$H_z^{scat}(x, y) = \sum_{e=1}^{N_e} H_z^{se} = \sum_{e=1}^{N_e} \sum_{i=1}^3 H_{zi}^{se} \cdot N_i^e(x, y), \quad (3)$$

where basis function for triangle e-th element that occupy region  $\Omega^e$  is:

$$N_i^e(x, y) = \begin{cases} a_i^e + b_i^e \cdot x + c_i^e \cdot y & \text{for } \bar{\mathbf{r}} \in \Omega^e; \\ 0, & \text{otherwise;} \end{cases}$$

$$a_i^e = \frac{x_j^e \cdot y_k^e - x_k^e \cdot y_j^e}{(x_2^e - x_1^e) \cdot (y_3^e - y_1^e) - (x_3^e - x_1^e) \cdot (y_2^e - y_1^e)};$$

$$b_i^e = \frac{y_j^e - y_k^e}{(x_2^e - x_1^e) \cdot (y_3^e - y_1^e) - (x_3^e - x_1^e) \cdot (y_2^e - y_1^e)};$$

$$c_i^e = \frac{x_k^e - x_j^e}{(x_2^e - x_1^e) \cdot (y_3^e - y_1^e) - (x_3^e - x_1^e) \cdot (y_2^e - y_1^e)}.$$

The coefficients are expressed by co-ordinate of e-th triangle.

We choose Galerkin testing ( $W \equiv N_j^e$ ) and obtain the element equations

$$\sum_{e=1}^{N_e} \sum_{i=1}^3 H_{zi}^{se} \cdot \iint_{\Omega_e} \left[ -\nabla N_j^e \cdot \nabla N_i^e + k_0^2 \cdot \varepsilon_r \cdot N_j^e \cdot N_i^e \right] \cdot ds + \quad (4)$$

$$+ \sum_{s=1}^{N_s} \int_{C_s} N_j^e \cdot [\bar{\mathbf{n}} \cdot \nabla H_z^{scat}] \cdot dl = \sum_{e=1}^{N_e} \iint_{\Omega_e} N_j^e \cdot f^e \cdot ds$$

for  $j=1,2,3$ .

Here  $N_s$  is number of triangular elements that have edge on surface of region or number nodes on boundary (author recommend to choose odd number).

It is easy to verify that a

$$\bar{\mathbf{n}} \cdot \nabla H_z^{scat} = \frac{\partial H_z^{scat}}{\partial n}$$

is normal derivative on region boundary.

Due to the orthogonality of testing functions, from (4) it is possible to obtain equations for every element of the mesh. Summing them we get equations for every node of the mesh. These equations lead to a system of equations with a sparse matrix. But this system is not solvable because unknown are the field intensity in every node and its normal derivative on the boundary. To truncate mesh on the boundary of FEM region we use BI conditions tying on boundary field and its normal derivatives [1]. The Boundary Integral Method for mesh truncating uses exact solution of contour integrals to calculate the scattered field in the point  $\bar{\mathbf{r}}$ :

$$H_z^{scat}(\vec{r})\Big|_{\vec{r} \in C} = -\oint_C \frac{\partial H_z(\vec{r}')}{\partial n'} \cdot G^{2D}(\vec{r}, \vec{r}') \cdot dl' + \oint_C [\vec{n}' \cdot \nabla' G^{2D}(\vec{r}, \vec{r}')] \cdot H_z(\vec{r}') \cdot dl', \quad (5)$$

where 2D Green function:

$$G^{2D}(\vec{r}, \vec{r}') = \frac{-i}{4} \cdot H_0^{(2)}(k \cdot |\vec{r} - \vec{r}'|).$$

Boundary equation (5) contains incident and scattered fields, which have to be separated

$$\begin{aligned} H_z^{scat}(\vec{r})\Big|_{\vec{r} \in C} + \oint_C \frac{\partial H_z^{scat}(\vec{r}')}{\partial n'} \cdot G^{2D}(\vec{r}, \vec{r}') \cdot dl' - \\ - \oint_C [\vec{n}' \cdot \nabla' G^{2D}(\vec{r}, \vec{r}')] \cdot H_z^{scat}(\vec{r}') \cdot dl' = \\ = \oint_C [\vec{n}' \cdot \nabla' G^{2D}(\vec{r}, \vec{r}')] \cdot H_z^i(\vec{r}') \cdot dl' - \\ - \oint_C \frac{\partial H_z^i(\vec{r}')}{\partial n'} \cdot G^{2D}(\vec{r}, \vec{r}') \cdot dl' = F(\vec{r}). \end{aligned} \quad (6)$$

For more compact subscript we use:

$$\frac{\partial H_z^{scat}(\vec{r})}{\partial n} = V(\vec{r}).$$

To solve (4) together with (6) in Galerkin basis we have to discretize (6). For unknown functions we employ the piecewise constant expansion on boundary

$$\begin{aligned} V &= \sum_{s=1}^{N_s} \frac{V_{s+1} + V_s}{2} \cdot P(\varphi - \varphi_{s \text{ mid}}); \\ H_z^{scat} &= \sum_{s=1}^{N_s} \frac{H_{z s+1}^{scat} + H_s^{scat}}{2} \cdot P(\varphi - \varphi_{s \text{ mid}}); \end{aligned}$$

where

$$P(\varphi - \varphi_{vid}) = \begin{cases} 1 & \text{for } |\varphi - \varphi_{vid}| < \Delta\varphi / 2; \\ 0, & \text{otherwise;} \end{cases}$$

where  $\Delta\varphi = 2\pi / N_s$ .

The region boundary and angles are sketched on Fig. 3.

3.

Now, for any boundary segment, values of the field and its normal derivatives are approximated with its average value at nodes. This approximation simplifies integrating for (6).

$$\begin{aligned} \frac{H_{zq}^{scat} + H_{zq+1}^{scat}}{2} + \sum_{s=1}^{N_s} \frac{V_s + V_{s+1}}{2} \cdot G_{sq} - \\ - \sum_{s=1}^{N_s} \frac{H_{zs}^{scat} + H_{zs+1}^{scat}}{2} \cdot G_{\nabla sq} = F(\vec{r}_q) \end{aligned} \quad (7)$$

for  $q=1, 2, \dots, N_s$

where

$$\begin{aligned} G_{sq} &= \frac{-i \cdot \rho}{4} \int_{\varphi_s - \Delta\varphi/2}^{\varphi_s + \Delta\varphi/2} H_0^{(2)} \left( 2 \cdot k_0 \rho \cdot \sin((\varphi_q - \varphi')/2) \right) \cdot d\varphi', \\ G_{\nabla sq} &= \frac{d}{dr} \cdot \int_{\varphi_s - \Delta\varphi/2}^{\varphi_s + \Delta\varphi/2} \left[ \frac{i \cdot \rho}{4} \cdot H_0^{(2)} \left( 2 \cdot k_0 \cdot r \cdot \sin((\varphi_q - \varphi')/2) \right) \cdot d\varphi' \right]_{r=\rho}. \end{aligned}$$

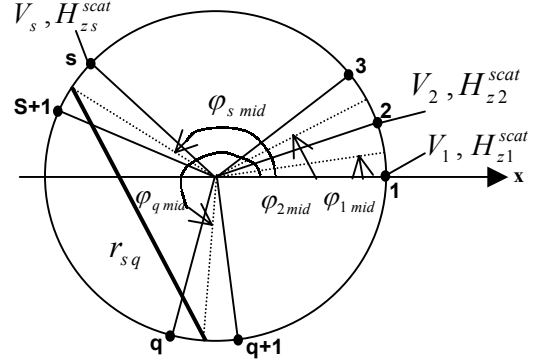


Fig. 3. Functions and angles on boundary of region

Now the assembled system (4) and (7) have to be solved and the field for every node in the region and its normal derivatives on boundary are determined.

On boundary most preferable is cylindrical system co-ordinate. For this case on  $r = \rho$ :

$$\frac{\partial H_{zs}^{scat}}{\partial r} = \frac{\partial H_{zs}^{scat}}{\partial n}; \quad \frac{1}{r} \frac{\partial H_{zs}^{scat}}{\partial \varphi} = \frac{H_{zs+1}^{scat} - H_{zs-1}^{scat}}{2 \cdot \Delta\varphi \cdot \rho}.$$

Now from Maxwell equations we can determine components of scattered electrical field:

$$E_r^{scat} = \frac{-i \cdot Z_0}{k_0 \cdot \varepsilon \cdot \rho} \cdot \frac{\partial H_z^{scat}}{\partial \varphi}; \quad E_\varphi^{scat} = \frac{i \cdot Z_0}{k_0 \cdot \varepsilon} \cdot \frac{\partial H_z^{scat}}{\partial r},$$

where  $Z_0$  - free room impedance.

The Pointing vector for scattered field

$$\begin{aligned} \vec{\Pi} &= 0.5 \cdot \vec{E}^{scat} \times \vec{e}_z \cdot H_z^{scat*} = \vec{e}_r \Pi_r - \vec{e}_\varphi \Pi_\varphi = \\ &= \vec{e}_r E_\varphi^{scat} \cdot H_z^{scat*} / 2 - \vec{e}_\varphi E_r^{scat} \cdot H_z^{scat*} / 2 \end{aligned}$$

Radiated power from the new ray is determined by real parts of the Pointing vector:

$$\Pi^{ray} = \sqrt{\text{Re}(\Pi_r) \cdot \text{Re}(\Pi_r) + \text{Re}(\Pi_\varphi) \cdot \text{Re}(\Pi_\varphi)}$$

and field intensity  $|H_z^{ray}| = \sqrt{2 \cdot \Pi^{ray} / Z_0}$ .

The new ray is located between angle  $\varphi_{s-1 \text{ mid}}$  and  $\varphi_{s \text{ mid}}$  (Fig. 4).

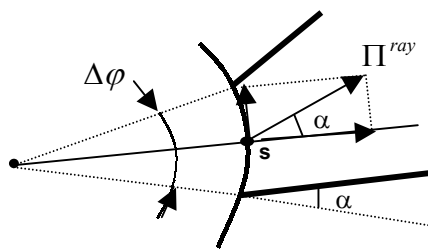


**Fig.4.** Secondary ray between bold lines:  $\alpha = a \tan(\Pi_\phi / \Pi_r)$  ;  
 $\beta$  - angle between x axis and s-the radius ( $\Pi_r$  ).

$$H_z^{ray} = |H_z^{ray}| \cdot \exp[-i \cdot k_0 \cdot (x \cdot \cos(\alpha + \beta) + y \cdot \sin(\alpha + \beta))].$$

The secondary rays are obtained from the Pointing vector of scattered field and its normal derivatives on the region boundary.

### Conclusion

This paper explains a combination of ray tracing and finite element methods. The Pointing vector of scattered field is obtained using boundary integral method for mesh

truncating. Some numerical results for hybrid method with secondary source are presented in paper [5].

### References

1. **Volakis J.L., Chatterjee A., Kempel L.C.** Finite Element Method for Electromagnetics. - IEEE Press, 1998.
2. **Taflov A.** Advances in Computational Electrodynamics. The Finite Difference Time Domain Method. - Artech House, 1998.
3. **Wang Y., Safavi-Naeini S., Chaudhuri K.** A hybrid technique based on Combining ray tracing and FDTD methods for site-specific modeling of indoor radio wave propagation // IEEE Transactions on Antennas and Propagation.- Vol 48, No.5, 2000.- P. 743-754.
4. **Ziemelis J.** Some Problems of ray tracing from indoor // Scientific proceeding of Riga Technical University. Telecommunications and Electronics.- Riga, 2001.- Vol. 7, No.1. - P. 20 -23.
5. **J.Ziemelis.** A hybrid method for ray tracing simulation. Conference Proceedings. Baltic Electronics Conference.- Tallin, October 6-9, 2002.. -P. 69-72.

Pateikta spaudai 2003 06 02

**J. Ziemelis. Bangų sklaidimo simuliacijos analizė remiantis baigtinių elementų teorija // Elektrotechnika ir elektrotechnika.- Kaunas: Technologija, 2003.- Nr. 5(47). – P. 65-68.**

Elektromagnetinio lauko simuliacijai apskaičiuoti siūloma taikyti mišrius metodus: spinduolio ir baigtinių elementų. Šiais dviem analizės metodais galima nustatyti lauko stiprumą sričių ribose ir orientacinę antrinių spinduliavimo elementų elektromagnetinio lauko dydį. Il.4, bibl.5 (anglų kalba; santraukos lietuvių, anglų ir rusų k.).

**J. Ziemelis. Problems of Secondary Sources for Hybrid Ray Tracing and FEM Simulation // Electronics and Electrical Engineering.- Kaunas: Technologija, 2003. – No. 5(47). – P. 65-68.**

The indoor propagation simulation of hybrid methods are employed. Usually for microwave band the hybrid method is based on ray tracing. In this case for numerical field calculation in regions with a small obstacles is selected finite element method (FEM). This paper explains solution method for two - dimensional FEM region with a boundary integral mesh truncating. Solving the system of FEM equations and boundary conditions, the field and its normal derivatives on boundary of region are determined. This solution gives orientation and field intensity for secondary source. Il 4, bibl. 5 (in English; summaries in Lithuanian, English, Russian).

**Ю. Зиемелис. Проблемы вторичных источников в гибридной программе симуляции распространения волн на базе лучевого метода и конечных элементов. // Электроника и электротехника. - Каунас: Технология. - 2003.- № 5(47). – С. 65-68.**

Для симуляции распространения электромагнитных волн в помещениях часто используются гибридные методы. В микроволновом диапазоне гибриды строятся на основе лучевого метода. В данном случае для расчета поля в областях с мелкими препятствиями выбран метод конечных элементов. Статья рассматривает двумерный модель с применением поверхностного интеграла для ограничения области. В результате совместного решения уравнений конечных элементов и поверхностных условий на границе области получаются напряженности поля и его нормальные производные, которые позволяют определить напряженность поля и ориентацию излучения вторичного источника. Ил. 4, библи. 5 (на английском языке; рефераты на литовском, английском и русском яз.).